Higher-moment singularities explored by net-proton nonstatistical fluctuations

Dai-Mei Zhou,[1] Ayut Limphirat,[2,5] Yu-liang Yan,[3] Cheng Yun,[1] Yu-peng Yan,[4,5] Xu Cai,[1]
Laszlo P. Csernai,[6,7] and Ben-Hao Sa[1,3,4]

[1]*Institute of Particle Physics, Central China Normal University, 430082 Wuhan, China and Key Laboratory of Quark and Lepton Physics (CCNU), Ministry of Education, China*

[2]*Department of Applied Physics, Faculty of Sciences and Liberal Arts, Rajamangala University of Technology Isan, Nakhon Ratchasima 30000, Thailand*

[3]*China Institute of Atomic Energy, P.O. Box 275 (10), 102413 Beijing, China*

[4]*School of Physics, Institute of Science, Suranaree University of Technology, Nakhon Ratchasima 30000, Thailand*

[5]*Thailand Center of Excellence in Physics (ThEP), Commission on Higher Education, Bangkok 10400, Thailand*

[6]*Department of Physics and Technology, University of Bergen, N-5007 Bergen, Norway*

[7]*Wigner Research Center for Physics, H-1525 Budapest, Pf. 49, Hungary*

(Received 25 May 2012; revised manuscript received 7 June 2012; published 27 June 2012)

We use the nonstatistical fluctuation to explore the higher-moment singularities of net-proton event distributions in the relativistic Au + Au collisions at $\sqrt{s_{NN}}$ from 11.5 to 200 GeV calculated by the parton and hadron cascade model PACIAE. The PACIAE results of mean (M), variance (σ^2), skewness (S), and kurtosis (κ) are consistent with the corresponding STAR data. Nonstatistical moments are calculated as the difference between the moments derived from real events and the ones from mixed events, which are constructed by combining particles randomly selected from different real events. An evidence of singularity at $\sqrt{s_{NN}} \sim 60$ GeV is first seen in the energy-dependent nonstatistical S and $S\sigma$.

DOI: 10.1103/PhysRevC.85.064916 PACS number(s): 25.75.Dw, 24.60.Ky, 24.10.Lx

I. INTRODUCTION

Describing the QCD phase diagram as a function of temperature T and baryon chemical potential μ_B is one of the fundamental goals of heavy-ion collision experiments [1]. The finite temperature lattice QCD calculation at $\mu_B = 0$ predicts that a crossover transition from the hadronic phase to quark gluon plasma (QGP) phase may occur at temperatures of 170–190 MeV [2,3]. However, a QCD-based model calculation indicates that the transition could be first order at large μ_B [4]. Once the location of the QCD critical point (QCP), where the phase transition proceeds from first order to crossover, is identified, the global structure of the phase diagram is known [5,6].

A characteristic feature of QCP is the divergence of the correlation length ξ [7] and the extremely large critical fluctuations [8]. In a static and infinite medium, various moments of conserved quantities such as the net-baryon, net-charge, and net-strangeness are related to the correlation length ξ [9]. Typically the variance (σ^2) of these distributions is related to ξ as $\sigma^2 \sim \xi^2$ [8]. It is pointed out in Ref. [10] that higher moments of conserved quantity event distributions, measuring deviations from a Gaussian, are sensitive to the QCP fluctuations.

In the first reference listed in Ref. [11] the hadron and quark-gluon coexisting phase, in a small volume, has been investigated with a simple effective model. Assuming this finite system was in a heat reservoir, the order parameter (energy density e) fluctuation near the phase transition was studied in a way similar to the Landau theory. A positive skewness (S) was predicted and a negative kurtosis (κ) was expected for the extensive thermodynamical quantities. In the second reference listed in Ref. [11] the dynamical change of skewness and kurtosis was analyzed during hadronization of QGP. It was shown that the skewness changes from negative to positive during the transition. While the kurtosis was positive in the initial dominantly QGP phase and after hadronization, it was negative during the process of transition. Similarly, it was predicted in the effective theory [10,12] that a crossing of the phase boundary may result in a change of sign of skewness as a function of the energy density. It was also reported recently that the sign of kurtosis could be negative as well, if the QCP is approached from the crossover side of the QCD phase transition [13].

The products of higher moments, such as $S\sigma$ and $\kappa\sigma^2$, are related to the ratio of conserved quantity number susceptibilities (χ): $S\sigma \sim \chi^{(3)}/\chi^{(2)}$ and $\kappa\sigma^2 \sim \chi^{(4)}/\chi^{(2)}$ [14]. It is predicted that the conserved quantity event distribution becomes non-Gaussian and the susceptibility diverges when QCP is approached. This causes $S\sigma$ and $\kappa\sigma^2$ to change significantly.

Recently, QCP and the higher moments of conserved quantity event distribution in heavy-ion collisions at BNL Relativistic Heavy Ion Collider (RHIC) energies have aroused further interest both experimentally [7,15,16] and theoretically [17–24]. On the experimental side, a method to determine T_c based on data has been proposed in Ref. [15]. By comparing the lattice results with the RHIC BES (Beam Energy Scan) fluctuation data of variance, skewness, and kurtosis systematically, the critical temperature has been determined to be $T_c = 175^{+1}_{-7}$ MeV. However, no evidence of singularity in energy dependence (at given centrality) and/or centrality dependence (at given energy) has been reported. On the other hand, copious models have been further proposed: such as the lattice QCD [17], the 2 + 1 flavor quark-meson model, the Polyakov quark-meson model [18], the

Polyakov-Nambu-Jona-Lasinio (PNJL) model [19,20], the Dyson-Schwinger equation [21], the statistical model [22,23], and the UrQMD and AMPT transport models [16,24], etc. Each model has its merits and results, but the consistency is lacking and contradiction exists among the theoretical models (cf. Fig. 4 in Ref. [7] for instance). The difficulty is that the fluid dynamical development of energy, momentum, and baryon charge density leads to a complex spatial distribution of the measured and statistically analyzed quantities at the freeze-out and hadronization domain of the space-time. These also influence the measured higher moments even without a phase transition, and disentangling the two effects is not easy [25]. Thus the question is still open and further studies are required.

In this paper a new method is studied to provide more insight. Namely, the nonstatistical moments of net-proton event distribution are calculated as the difference between the moments derived from real events generated by the parton and hadron cascade model PACIAE [26] and the ones from mixed events [27] which are randomly constructed according to the real events. In this way the single particle distribution arising from the fluid dynamic development is separated from the two and more particle correlations stemming from the PACIAE model where the hadronization and freeze-out take place, according to our expectation.

II. MODELS

The PACIAE model [26] is a parton and hadron cascade model, which is based on PYTHIA [28]. PACIAE consists of four stages: parton initiation, parton evolution (rescattering), hadronization, and hadron evolution (rescattering).

In the parton initiation stage, a nucleus-nucleus collision is decomposed into binary nucleon-nucleon (NN) collisions according to the collision geometry and total NN cross section. The collision time is calculated for each NN collision pair assuming a straight line trajectory between two consecutive NN collisions and the NN collision list is then constructed by all collision pairs. A NN collision with earliest collision time is selected from the collision list and performed by PYTHIA with string fragmentation switched off, and diquarks (anti-diquarks) broken into quark pairs (antiquark pairs). Thus a parton initial state (quarks, antiquarks, and gluons) is eventually obtained when NN collision pairs are exhausted.

The parton rescattering is then proceeded by the Monte Carlo method using $2 \to 2$ leading order perturbative QCD cross sections [29]. The parton evolution stage is followed by the hadronization at the moment of partonic freeze-out (exhausting the partonic collisions). The Lund string fragmentation model and a phenomenological coalescence model are provided for hadronization. After this the rescattering among produced hadrons is dealt with the usual two-body collision model [26]. Only the rescatterings among π, K, p, n, $\rho(\omega)$, Δ, Λ, Σ, Ξ, Ω, J/Ψ, and their antiparticles are considered for simplicity.

Like other transport (cascade) models, such as the above-mentioned UrQMD [30] and/or AMPT [31], PACIAE does not assume equilibrium. It just simulates dynamically the whole relativistic heavy-ion collision process from the initial partonic stage to the hadronic final state via the parton evolution (not implemented in UrQMD), hadronization, and hadron evolution according to copious dynamical ingredients (assumptions) introduced reasonably. Therefore it is parallel to the experimental nucleus-nucleus collision. These dynamics correctly describe the particle, energy, and entropy developments, etc., while the intensive thermodynamical quantities are not defined in this nonequilibrium regime. Messages brought by the produced particles in these transport (cascade) models are all of dynamical origin. Unlike most of the hydrodynamic models where the phase transition is described via the assumptions for equations of state, in PACIAE (the same in UrQMD and/or AMPT) we do not implement a phase transition congenitally. However, once there is a phase transition signal in transport (cascade) model calculations, it must be a result of dynamical evolution. Of course, further studies are then required.

The nth moment about the mean of a conserved quantity, x, with the event distribution $P(x)$ is expressed as

$$M^{(n)} = \langle (x - \langle x \rangle)^n \rangle = \int (x - \langle x \rangle)^n P(x) dx, \tag{1}$$

where the nth moment around zero reads as

$$\langle x^{(n)} \rangle = \int x^n P(x) dx. \tag{2}$$

The higher moments as well as their products investigated widely are then the following:

$$\text{variance,} \quad \sigma^2 = M^{(2)}; \tag{3}$$

$$\text{skewness,} \quad S = M^{(3)}/(M^{(2)})^{3/2}; \tag{4}$$

$$\text{kurtosis,} \quad \kappa = M^{(4)}/(M^{(2)})^2 - 3, \tag{5}$$

$$S\sigma = M^{(3)}/M^{(2)}, \tag{6}$$

and

$$\kappa\sigma^2 = M^{(4)}/M^{(2)} - 3M^{(2)}, \tag{7}$$

besides the mean $M \equiv \langle x^{(1)} \rangle$ and $M^{(1)} \equiv 0$.

The study of higher-moment singularities is a matter of dynamics, but the statistical fluctuation is always dominant. Therefore, we study the nonstatistical part of fluctuations instead of full fluctuations in this paper. The parton and hadron cascade model PACIAE [26] is applied to generate real events. Each real event obeys dynamical conservation laws (such as net-baryon number conservation, energy and momentum conservation, etc.), which cause the correlations among particles in a single event. As the PACIAE model simulation for a nucleus-nucleus collision is parallel to the experiment of a nucleus-nucleus collision, the NA49 method [27] is also employed to generate the mixed events. This means that the mixed events are constructed by combining particles randomly selected from different real events, while reproducing the event multiplicity distribution of real events. We have checked that the dynamical conservation laws really do not exist in the mixed event and there are only statistical fluctuations caused by the effects of finite event number, finite size, and experimental finite detector resolutions. The nonstatistical moments of conserved quantity event distributions are defined to be the difference between the moments derived from real events and the ones from mixed events. Thus the

dynamical fluctuations are pronounced from the underlying dominant statistical fluctuations and are expected to be seen easily in the nonstatistical higher moments.

If the nth moment around the mean calculated by real (mixed) events is denoted by $M_R^{(n)}$ ($M_M^{(n)}$), then the corresponding nth nonstatistical moment around the mean, like in Ref. [27], is

$$M_{\rm NON}^{(n)} = M_R^{(n)} - M_M^{(n)}. \quad (8)$$

III. RESULTS

The net-proton event distribution and the corresponding higher moments in relativistic Au + Au collisions at $\sqrt{s_{NN}}$ from 11.5 to 200 GeV are calculated with both the PACIAE real events and the corresponding mixed events. It is found that the PACIAE results of mean, variance, skewness, and kurtosis in Au + Au collisions are in agreement with the STAR data. The STAR data on net-proton multiplicity distribution is not corrected for event-by-event proton and antiproton counting efficiency. The PACIAE model results do not incorporate this efficiency effect. It is expected that the effect of efficiency on products of moments is small [7].

Shown, as an example, in Fig. 1 are the results of PACIAE real events (open symbols) compared with the STAR data (solid symbols) of the net-proton event distribution in 0–5% most central Au + Au collisions at $\sqrt{s_{NN}} = 39$ GeV. Note that the spectator protons have been excluded here. One sees from Fig. 1 that the agreement between the STAR data and the PACIAE results is satisfactory: with two distributions having nearly the same peak location and close to each other until the half height. The deviation of the two distributions gets visible around the tails; however, the contribution of the tails to the moments is expected to be very small as the corresponding probability is rather low. To our knowledge there has not yet been a comparison between the STAR data of net-proton event

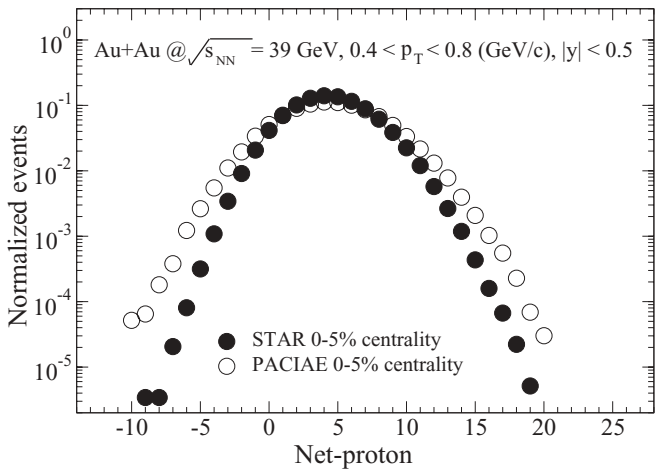

FIG. 1. Net-proton event distributions in Au + Au collisions at $\sqrt{s_{NN}} = 39$ GeV. The solid and open symbols are STAR data (taken from the first reference listed in Ref. [16]) and the results of PACIAE real events, respectively.

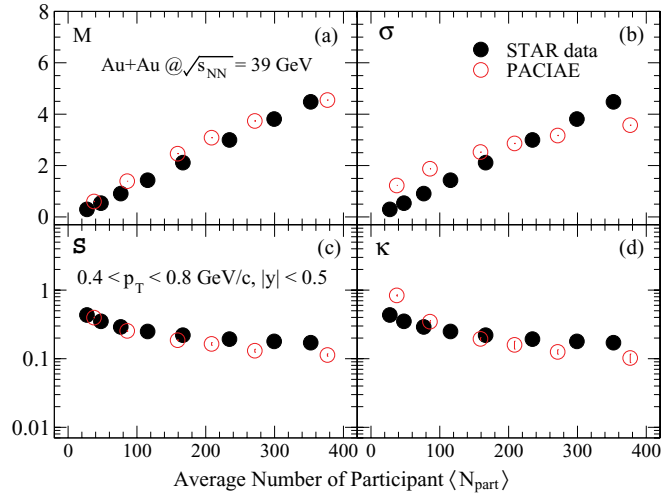

FIG. 2. (Color online) Centrality-dependent moments of net-proton event distribution in Au + Au collisions at $\sqrt{s_{NN}} = 39$ GeV. The solid and open circles are STAR data (taken from the first reference listed in Ref. [16]) and the results of PACIAE real events, respectively.

distribution and model calculations, except the parameter fit in Ref. [22].

The centrality-dependent STAR data of the moments of net-proton event distribution in Au + Au collisions at $\sqrt{s_{NN}} =$ 39 GeV (cf. first reference listed in Ref. [16]) are compared with the results of PACIAE real events in Fig. 2. In PACIAE the collision centrality is represented with the impact parameter b which is mapped to the experimental centrality in percentage (g) [32] by

$$b = \sqrt{g} b_{\rm max}, \quad b_{\rm max} = R_A + R_B. \quad (9)$$

Then the corresponding average number of participant nucleons is calculated by the geometric method and/or the Glauber model, we refer to the first reference listed in Ref. [26] for the details. One sees in this figure the agreement between the STAR data and the PACIAE results for M and S. However, the agreement for σ and κ is not as good as that for M and S. This reveals that the tails of the net-proton event distribution affect the even moments greatly.

Figure 3 shows the energy dependence of the STAR $\kappa\sigma^2$ data [7] (solid circles) and the results of PACIAE real events (open circles) in Au + Au collisions. In this figure the open triangles and the dashed line are the results of UrQMD and hadronic resonance gas (HRG) from Ref. [7], respectively. The STAR data of almost-energy-independent $\kappa\sigma^2$ is well reproduced by the HRG, approximately described by PACIAE within the error bars, but is not well reproduced by UrQMD. The error bar in the PACIAE results is estimated by repeating first the simulation six times independently (with different seeds of random numbers) and then calculating the standard variance of the observable [33].

We show in Fig. 4 the PACIAE results of energy dependence of the nonstatistical skewness [panel (a)], kurtosis [panel (b)], $S\sigma$ [panel (c)], and $\kappa\sigma^2$ [panel (d)] calculated for the 0–5% most central Au + Au collisions in the STAR acceptances of

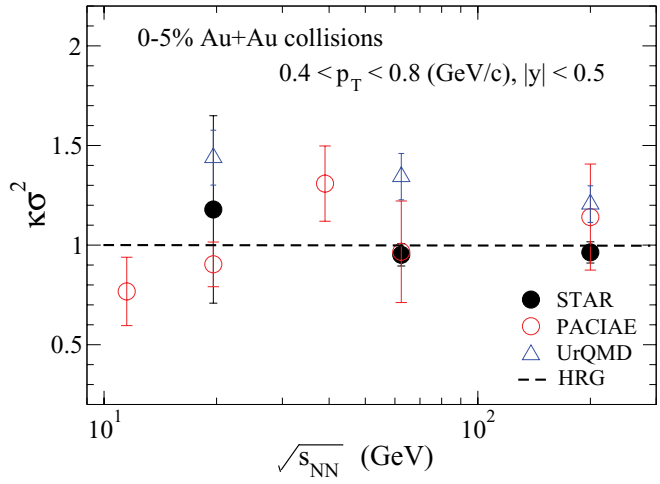

FIG. 3. (Color online) Energy dependence of $\kappa\sigma^2$ of net-proton event distribution in Au + Au collisions. The solid circles, the open circles, the open triangles, and the dashed line are the STAR data (taken from Ref. [7]), the results of PACIAE real events, the results of UrQMD (taken from Ref. [7]), and the results of HRG, respectively.

$|y| < 0.5$ and $0.4 < p_T < 0.8$ GeV/c according to Eqs. (1)–(8). The energies applied in the calculations are $\sqrt{s_{NN}} = 11.5$, 19.6, 39, 62.4, and 200 GeV, with the total number of generated real events being 3.0×10^5, 3.0×10^5, 2.4×10^5, 1.2×10^5, and 1.2×10^5, respectively. The same number of mixed events is then constructed correspondingly. It is found in this figure that the nonstatistical S, κ, $S\sigma$, and $\kappa\sigma^2$ change sign at $\sqrt{s_{NN}} \sim 60$ GeV. Here a first evidence of singularity is seen in the energy-dependent S and $S\sigma$. These signs, of course, are not seen in the results calculated by mixed events. They also do not show up in the results calculated by real events and in the STAR data (results of full fluctuations indeed) [15,34], because the dynamical fluctuations are always submerged in the statistical fluctuations. Thus the higher-moment singularity may be only implicated in the nonstatistical fluctuation.

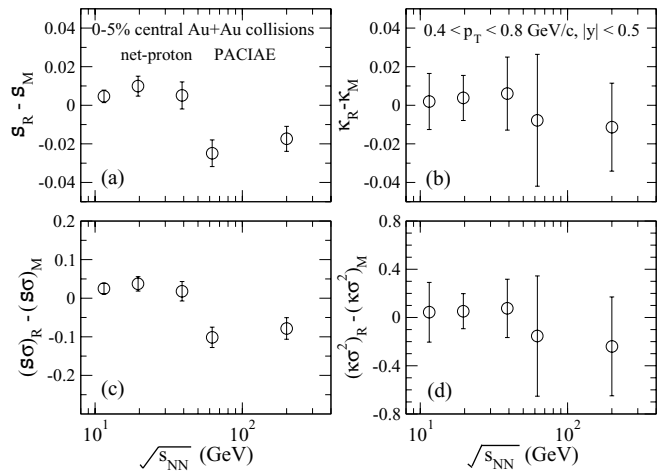

FIG. 4. Energy dependence of nonstatistical higher moments and their products of the net-proton event distribution in 0–5% most central Au + Au collisions.

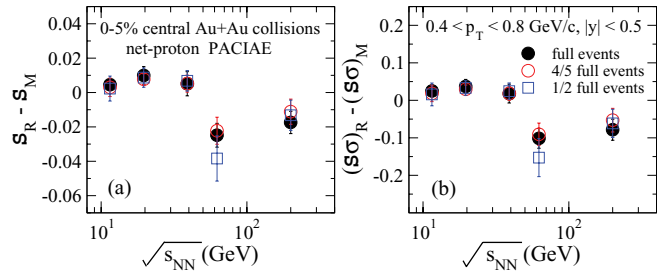

FIG. 5. (Color online) Energy dependence of nonstatistical S and $S\sigma$ of the net-proton event distribution in 0–5% most central Au + Au collisions.

The results in Fig. 4, when compared to the estimates in the second reference listed in Ref. [11], indicate that the freeze-out point is very close to the hadronization point as the value of skewness is rather small. Furthermore, at lower beam energies the skewness is positive, indicating a freeze-out closer to the QGP side in the hadronization process. But at higher beam energies the skewness is negative, indicating more dominance of the hadronic side of the phase transition. The kurtosis becomes significantly negative, although small at higher beam energies, indicating that the freeze-out is indeed in the phase transition domain. Since a number of dynamical ingredients are introduced in the PACIAE (PYTHIA) model, the detailed roles and effects of the dynamical ingredients relevant to this phenomenon have to be studied later.

To check the reliability of the sign changes in Fig. 4, we have recalculated the energy-dependent nonstatistical S and $S\sigma$ with 1/2 and 4/5 total number of events and compared the results with the ones calculated with the full number of events, as shown in Fig 5. We see in this figure that the convergence is quite good for $\sqrt{s_{NN}} = 11.5$, 19.6, 39, and 200 GeV and satisfactory for 62.4 GeV. Thus the results shown in Fig. 4 are reliable. The sign changes of S and $S\sigma$ shown in this figure may be a response to the prediction in Ref. [12].

IV. CONCLUSION

In summary, we have calculated the higher moments of net-proton event distributions in relativistic Au + Au collisions at $\sqrt{s_{NN}}$ from 11.5 to 200 GeV with real events generated by the parton and hadron cascade model PACIAE [26]. The PACIAE results of centrality-dependent net-proton M, σ, S, and κ in Au + Au collisions are consistent with the STAR data.

We have studied the nonstatistical fluctuations of net-proton event distributions. The mixed events are constructed according to PACIAE real events and the nonstatistical moments are calculated as the difference between the moments calculated from real events and those calculated from mixed events. The nonstatistical S, κ, $S\sigma$, and $\kappa\sigma^2$ appear to change signs at $\sqrt{s_{NN}} \sim 60$ GeV. The clear sign change in the energy-dependent nonstatistical S and $S\sigma$ may reflect some singularities. However, this has to be confirmed by the STAR Beam Energy Scan nonstatistical fluctuation data later. Thus, all of the comparisons between experiment and theory in this paper are preliminary.

ACKNOWLEDGMENTS

This work was supported by the National Natural Science Foundation of China under Grants No. 10975062, No. 11075217, No. 11105227, and No. 11175070 and by the 111 Project of the Foreign Expert Bureau of China. AL and YPY acknowledge financial support from TRF-CHE-RMUTI under Contract No. MRG5480186. The authors thank X. F. Luo for the STAR data. We are grateful to N. Xu for valuable discussions.

[1] J. Adams *et al*. (STAR Collaboration), Nucl. Phys. A **757**, 102 (2005); B. Mohanty, New J. Phys. **13**, 065031 (2011).

[2] Y. Aoki, G. Endrodi, Z. Fodor, S. D. Katz, and K. K. Szabo, Nature (London) **443**, 675 (2006).

[3] Y. Aoki, Z. Fodor, S. D. Katz, and K. K. Szabo, Phys. Lett. B **643**, 46 (2006); M. Cheng *et al*., Phys. Rev. D **74**, 054507 (2006).

[4] E. S. Bowman and J. I. Kapusta, Phys. Rev. C **79**, 015202 (2009); S. Ejiri, Phys. Rev. D **78**, 074507 (2008).

[5] M. A. Stephanov, Prog. Theor. Phys. Suppl. **153**, 139 (2004); Z. Fodor and S. D. Katz, J. High Energy Phys. 04 (2004) 050.

[6] R. V. Gavai and S. Gupta, Phys. Rev. D **71**, 114014 (2005); **78**, 114503 (2008).

[7] M. M. Aggarwal *et al*. (STAR Collaboration), Phys. Rev. Lett. **105**, 022302 (2010).

[8] M. A. Stephanov, K. Rajagopal, and E. Shuryak, Phys. Rev. D **60**, 114028 (1999).

[9] V. Koch, A. Majumder, and J. Randrup, Phys. Rev. Lett. **95**, 182301 (2005); M. Asakawa, U. Heinz, and B. Müller, *ibid*. **85**, 2072 (2000).

[10] M. A. Stephanov, Phys. Rev. Lett. **102**, 032301 (2009).

[11] L. P. Csernai and Z. Neda, Phys. Lett. B **337**, 25 (1994); L. P. Csernai, Z. Neda, and G. Mocanu, arXiv:1204.6394.

[12] M. Asakawa, S. Ejiri, and M. Kitazawa, Phys. Rev. Lett. **103**, 262301 (2009).

[13] M. A. Stephanov, Phys. Rev. Lett. **107**, 052301 (2011).

[14] M. Cheng *et al*., Phys. Rev. D **79**, 074505 (2009); F. Karsch and K. Redlich, Phys. Lett. B **695**, 136 (2011); R. V. Gavai and S. Gupta, *ibid*. **696**, 259 (2011).

[15] S. Gupta, X. Luo, B. Mohanty, H. G. Ritter, and X. Nu, Science **332**, 1525 (2011).

[16] X. Luo (STAR Collaboration), J. Phys.: Conf. Ser. **316**, 012003 (2011); Acta Phys. Pol. B: Proc. Suppl. **5**, 497 (2012); B. Mohanty, J. Phys. G: Nucl. Part. Phys. **38**, 124023 (2011).

[17] F. Karsch and K. Redlich, arXiv:1107.1412; R. V. Gavai, in Proceedings of Strangeness in Quark Matter, Krakow, September 18–24, 2011 (to be published in Acta Phys. Pol. B).

[18] B.-J. Schaefer and M. Wagner, Phys. Rev. D **85**, 034027 (2012).

[19] P. Costa, C. A. De Sousa, and M. C. Ruivo, arXiv:1112.6306.

[20] W.-J. Fu, Y.-X. Liu, and Y.-L. Wu, Phys. Rev. D **81**, 014028 (2010).

[21] S.-X. Qin, L. Chang, H. Chen, Y.-X. Liu, and C. D. Roberts, Phys. Rev. Lett. **106**, 172301 (2011).

[22] C. B. Yang and X. Wang, Phys. Rev. C **84**, 064908 (2011).

[23] P. Braun-Munzinger, B. Friman, F. Karsch, K. Redlich, and V. Skokov, Nucl. Phys. A **880**, 48 (2012).

[24] L. Chen, X. Pan, F. Xiong, L. Li, N. Li, Z. Li, G. Wang, and Y. Wu, J. Phys. G: Nucl. Part. Phys. **38**, 115004 (2011).

[25] D. J. Wang, L. P. Csernai, D. Strottman, Cs. Anderlik, Y. Cheng, D. M. Zhou, Y. L. Yan, X. Cai, and B. H. Sa, arXiv:1205.4934.

[26] B.-H. Sa, D.-M. Zhou, Y.-L. Yan, X.-M. Li, S.-Q. Feng, B.-G. Dong, and X. Cai, Comput. Phys. Commun. **183**, 333 (2012); Y.-L. Yan, D.-M. Zhou, B.-G. Dong, X.-M. Li, H.-L. Ma, and B.-H. Sa, Phys. Rev. C **79**, 054902 (2009); D.-M. Zhou, A. Limphirat, Y.-L. Yan, X.-M. Li, Y.-P. Yan, and B.-H. Sa, Phys. Lett. B **694**, 435 (2011).

[27] S. V. Afanasiev *et al*. (NA49 Collaboration), Phys. Rev. Lett. **86**, 1965 (2001); C. Alt *et al*. (NA49 Collaboration), Phys. Rev. C **79**, 044910 (2009); T. Anticic *et al*. (NA49 Collaboration), *ibid*. **83**, 061902 (2011).

[28] T. Sjöstrand, S. Mrenna, and P. Skands, J. High Energy Phys. 05 (2006) 026.

[29] B. L. Combridge, J. Kripfgang, and J. Ranft, Phys. Lett. B **70**, 234 (1977).

[30] S. A. Bass *et al*., Prog. Part. Nucl. Phys. **41**, 255 (1998).

[31] Z.-W. Lin, C. M. Ko, B.-A. Li, B. Zhang, and S. Pal, Phys. Rev. C **72**, 064901 (2005).

[32] B.-H. Sa, A. Bonasera, A. Tai, and D.-M. Zhou, Phys. Lett. B **537**, 268 (2002), and first quotation of Ref. [26].

[33] L. Lyons, *Statistics for Nuclear and Particle Physics* (Cambridge University Press, Cambridge, UK, 1986).

[34] X. Luo (STAR Collaboration), in Proceedings of the 7th International Workshop on Critical Point and Onset of Deconfinement, November 7–11, 2011, Wuhan, China.